

Controllable suppression of Non-Hermitian skin effects

Chao Xu¹, Zhiqiang Guan^{1,2,3,4*} and Hongxing Xu^{1,2,4*}

¹School of Physics and Technology, Center for Nanoscience and Nanotechnology, and Key Laboratory of Artificial Micro- and Nano-structures of Ministry of Education, Wuhan University, Wuhan 430072, China

²School of Microelectronics, Wuhan University, Wuhan 430072, China

³Hubei Yangtze Memory Laboratories, Wuhan 430205, China

⁴Wuhan Institute of Quantum Technology, Wuhan 430206, China

Abstract

The Non-Hermitian skin effect (NHSE) is a phenomenon in which the bulk states tends to the boundary in Non-Hermitian Hamiltonian, and has a wide range of application scenarios. The fully understanding of the skin mode anomalies in NHSEs is vital for the application. Recently, some innovative work reported the suppression [Phys. Rev. Lett 127, 256402 (2021)] and enhancement [Phys. Rev. Lett 131, 116601 (2023)] of NHSEs by magnetic field, respectively. In our work, we constructed magnetic field-like onsite potential energy distribution and random-like onsite potential energy distribution, and found that onsite potential energy has non-monotonic and monotonic suppression patterns on skin modes. Non-monotonic and monotonic suppression patterns are two typical forms in the transition from order to disorder. Only relying on onsite potential energy, not only we have obtained a profound understanding of the connection and difference between order and disorder, but also developed a general strategy to achieve both robustness and adjustability of the skin modes. By linking with the scaling theory in disorder, the controllable suppression of NHSEs, based on mutual transformation between order and disorder, is generalized to higher dimensions.

Introduction --- Compared to Hermitian systems, Non-Hermitian systems may have non-real eigenvalues[1-5], non-orthogonal eigenvectors[6-8], and Exceptional Points (EPs)[9-16], thus showing fruitful phenomena. A significant and widespread property of Non-Hermitian systems, characterized by topological invariants winding numbers, is the NHSE[17-25]. NHSE is a phenomenon that a system with non-zero winding numbers under the period boundary conditions (PBCs) will exhibit bulk states tending towards the boundary under open boundary conditions (OBCs)[26-31]. The necessary and sufficient conditions for non-zero winding numbers respect to a reference point can exist is that the energy eigenvalues form a closed curve with a certain interior on the energy complex plane under PBCs [32, 33]. The winding numbers compared to other topological invariants can be defined on a single energy band in one-dimension. Due to the universality of the Non-Hermitian system in the real world and the low requirement for defining winding numbers, compared to other Non-Hermitian topological physics, the NHSEs have important practical value. When there are higher dimensions, more symmetries, or more complex

systems, winding numbers will have richer connotations[34-37]. The NHSEs has been observed in many systems, including optical, acoustic, electric circuit, quantum walk and synthetic dimensions[38-47].

Although there have been many theoretical and experimental studies on the NHSEs[38-50], there are still some abnormal skin mode suppression/enhancement and geometry-dependent skin effects that may occur[32, 51-56]. The unified theoretical explanation for these anomalies is very challenging. In depth study of NHSEs, theoretically speaking, there are only two sources for the generation of skin modes, one is onsite potential energy and the other is hopping term. This work mainly focuses on onsite potential energy. There are not many direct studies related to potential energy, but the effects of many specific physical fields can be manifested as potential energy, such as electric[51] and magnetic fields[52, 56]. These indirect studies are not systematical and have not accurately revealed the complete patterns of skin mode suppression. There were some innovative researches on the effects of magnetic fields on NHSEs, and magnetic fields can be regarded as a presentation form of potential energy. They discovered a competitive relationship between magnetic fields and Non-Hermitian[52], namely nonperturbative nature of magnetic fields that magnetic fields is prone to localize states within the bulk, and skin nature of Non-Hermitian. As the magnetic field increases, some skin modes are suppressed and returned to the bulk[52]. But also existing work studying the enhancement the second-order Non-Hermitian skin effects by magnetic field[56]. So there are two questions how the magnetic field effect the skin modes, and can we regulate them?

In this work, we constructed magnetic field-like onsite potential and random-like onsite potential based on previous works, and found that onsite potential energy has non-monotonic and monotonic suppression patterns on skin modes, paving a novel path for regulating the skin modes. In the one-dimensional nearest-neighbor non-reciprocal hopping Hatano-Nelson model with considering periodic onsite potential energy, we first constructed a magnetic field-like potential energy distribution based on the Hofstadter model, then discovered suppression of skin mode first increases and then decreases with the increase of magnetic field, simultaneously modulated by the lattice. Starting from the perspective of electron tunneling within potential barriers, we speculate that there is a non-monotonic relationship between barrier disorder introduced by magnetic field and magnetic field intensity. To verify the hypothesis, we first need to extract the general relationship between (more general) barrier disorder and period as much as possible, because the magnetic field intensity is inversely proportional to the onsite potential period. Then we constructed a random-like onsite potential energy distribution, and discovered monotonic suppression patterns. Non-monotonic and monotonic suppression patterns are two typical forms for order and disorder, respectively. Solely from the onsite potential energy, not only we gained a profound understanding of the connection and difference between order and disorder, but also we developed a general strategy to control skin mode suppression. Finally, by combining with the scaling theory in disorder, the controllable suppression of skin modes, based on mutual transformation between order and disorder, is generalized to higher dimensions.

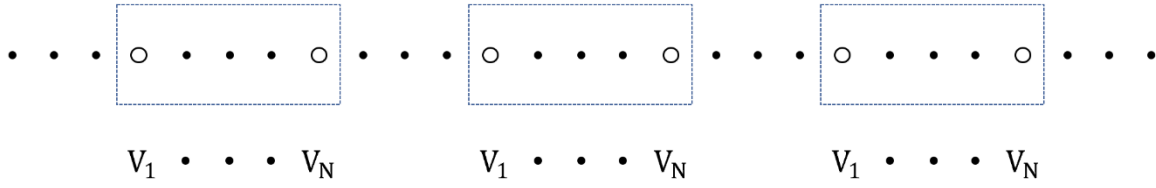


Fig.1 Schematic diagram of a one-dimensional single-atom chain considering onsite energies with period N .

Non-monotonic suppression by magnetic field --- The study of NHSEs can start with the most basic one-dimensional single atom model. Non-Hermitian Hamiltonians often involve non-reciprocal hopping terms or complex onsite energy, complex onsite energy includes gain and loss at sites. For simplicity and representativeness, we start with the simplest case, considering only the nearest-neighbor hoppings with periodic onsite potential energies, the Hamiltonian can be written as

$$\hat{H} = \sum_i t_{-1} \hat{a}_i^\dagger \hat{a}_{i+1} + t_{+1} \hat{a}_{i+1}^\dagger \hat{a}_i + \sum_i V_{i \bmod N} \hat{a}_i^\dagger \hat{a}_i \quad (1)$$

t_{-}, t_{+} are the hopping amplitude towards left and towards right, respectively. $V_{i \bmod N}$ is onsite potential energy at site i with period N , schematic diagram shown as in Fig.1.

Consider a single electron in a non-reciprocal hopping square lattice with a vertical magnetic field applied, namely, Non-Hermitian Hofstadter model. The Hermitian Hofstadter model has a butterfly-shaped energy spectrum[57], which is also a classical quantum fractal model in physics, satisfying the Streda formula[58] and Wannier's Diophantine equation[59]. The core feature of the Hofstadter model is the possession of a magnetic translation group[60]. The Hofstadter model studies the competitive relationship between magnetic field and lattice, which may also be used to investigate the relationship between onsite potential energy and lattice. The Peierls substitution[61] is taken along the x -axis direction, the magnetic flux per unit cell $\phi = 2\pi \frac{p}{q}$, where p, q are coprime, t_x is the x -axis direction nearest-neighbor hopping amplitude, t_y^- and t_y^+ are the y -axis direction nearest-neighbor downward and upward hopping amplitudes. When x -axis direction takes the PBCs, its Hamiltonian can be written as

$$\hat{H} = \sum_{k_x, n} (t_x e^{-ik_x + i\phi n} \hat{a}_n^\dagger \hat{a}_n + t_x e^{+ik_x - i\phi n} \hat{a}_n^\dagger \hat{a}_n + t_y^+ \hat{a}_{n+1}^\dagger \hat{a}_n + t_y^- \hat{a}_n^\dagger \hat{a}_{n+1}) \quad (2)$$

Non-reciprocal hopping terms do not break the magnetic translation group. It is obvious that the Hamiltonian at certain k_x is equivalent to a one-dimensional single-atom chain considering onsite potential energies with period q to some degree and its onsite potential distribution obeys a cosine function distribution. The Hofstadter model is an important platform for studying the novel Hall effects[62]. Since there are works having been done to generalize the Chern numbers from Hermitian Hamiltonian to non-Hermitian ones[29], the non-Hermitian Hofstadter model can still define the non-trivial Chern numbers and obtain topological edge states, however, it is not impossible to give a quantitative relationship between the non-Hermitian strength and the Chern numbers analytically because this model often lacks an analytic solution. (More information on the energy bands and state distribution of the

Hofstadter model can be found in the supplementary materials, Sec. I).

Taking $k_x = 0$, 500 atoms in the y -axis, the distribution of states are calculated in Fig.2 as p/q increasing. Reasonable setting of simulation parameters can make the topological edge states only appear on right side. In panel (a), (b), and (c), the three states with the lowest energy were selected in color. It can be seen when there is no magnetic field, the skin mode tends towards the boundary. As the magnetic field increases, some skin modes enter the body, namely the anti-skin modes. Then, we choose an appropriate magnetic field intensity so that the magnetic field forms exactly two or three wave packets in spatial distribution in panel (c), (d), (e). Further increasing the magnetic field, the skin modes re-tend to the boundary, as shown in panel (f). This is not entirely consistent with previous work which only reveal the exceptionally robust magnetic confinement effect that counteracts non-Hermiticity[52]. The popular physical image of magnetic confinement effect is the localization of electrons under the Lorentz force. We believe that this view is not appropriate. In our work, the magnetic field (intensity is proportional to $\frac{p}{q}$) can be regarded as a potential barrier for electrons to hop. When

the magnetic field is zero, the electron hopping is unobstructed by the potential barrier, and the skin modes normally concentrate to the boundary. As the magnetic field intensity increases, the potential barrier hinders the electron hopping, and some skin modes enter the bulk. As the magnetic field intensity continues to increase, the space period $\frac{q}{p}$ from magnetic field decreases.

When the variance of the barrier distribution remains roughly unchanged, a decrease in the period is beneficial for electron tunneling, and the skin modes gradually return to the boundary. We also chose a triangle onsite potential distribution and observed similar phenomena (see supplementary materials, Sec. III)

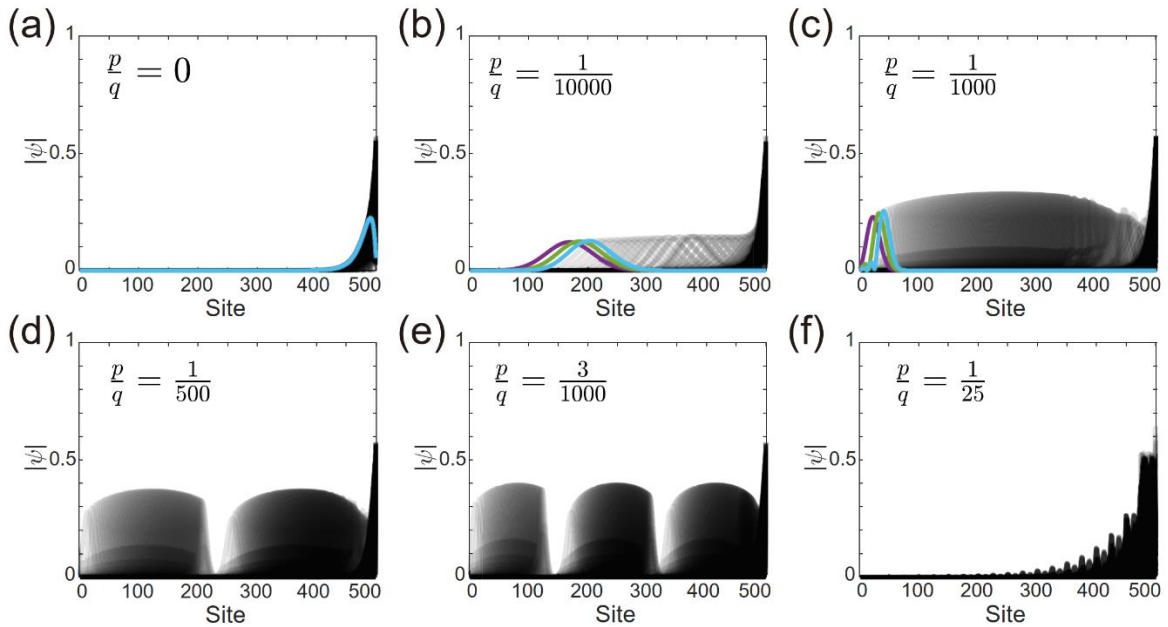


Fig.2 Skin modes suppression in Hofstadter model. Take $k_x = 0$, 500 atoms in the y-axis, and calculate state distribution under $t_x = 1, t_y^- = 0.9, t_y^+ = 1.1$. The three lowest energy states are marked in color in (a), (b), (c).

Monotonic suppression with random potential energy --- In a finite chain, the suppression pattern of skin modes depend on the relationship between the disorder strength and the period, but it is difficult for the conventional distribution period of onsite energies to decouple the two. We need a better system to analyze the relationships between them as much as possible. We choose a one-dimensional single atomic added with periodic random onsite energy. If the period N is equal the total number L of chain atoms, this model will degenerate the Non-Hermitian Anderson model[63-66]. If the period N is equal to 1, this model will be a Non-Hermitian Hatano-Nelson model with a constant onsite potential energy distribution. We simulated the anti-skin mode proportion in a total number of atoms of $L = 400$, sampling 100 times under different periods N and disorder amplitude W , it is found that the anti-skin mode are basically positively correlated as the period and disorder amplitude increases, as shown in Fig.3 (More details about wavefunction distribution under disorder in Supplementary Materials, Sec. IV). In a finite chain, when the disorder amplitude W is determined, and the period N increases from 1 to the total atoms number L , which is equivalent to the constant potential energy Hatano-Nelson model gradually transitioning to the Anderson model, and the disorder strength will continue to increase, resulting in an increase in the proportion of anti-skin mode. When the period N is determined, the disorder amplitude W increases, and similar to the Anderson model, the disorder strength also increases continuously. Due to the randomness of onsite energy, there may be some error in the anti-skin mode proportion.

Compared to the previous cosine onsite energy distribution or triangular onsite energy distribution, random onsite energy can better decouple disorder strength and period N as much as possible, but it is not completely decoupled either. The disorder amplitude W and period N of the onsite energy can be regarded as components of disorder strength. In the Anderson model, the higher the disorder degree, the more localized the state distribution is. Although Anderson localization is aimed at disordered localization, and cosine and other onsite energy distributions are not random distributions, the principle is the same. There are at least two reasons. Firstly, according to the Fourier transform, any period function can be viewed as a linear superposition of many sine (cosine) functions; Secondly, a large amount of work has been done to combine the NHSEs with the Anderson localization, expanding the phase transition from the extended states to the localized states in the Anderson localization to the skin modes to the anti-skin modes[67-69].

The closer the coupling between the disorder strength and the period N (or the more the potential barrier distribution tends to be a simple function distribution), the more the skin mode suppression shows a pattern of first strengthening and then weakening as the periodic independent variable (such as magnetic field strength) increases. On the contrary, if the coupling is not tight, it will continue to strengthen with the increase of the periodic independent variable until all are localized within the bulk. By controlling the onsite energy distribution function, an interesting strategy to control suppression pattern of skin modes can be obtained.

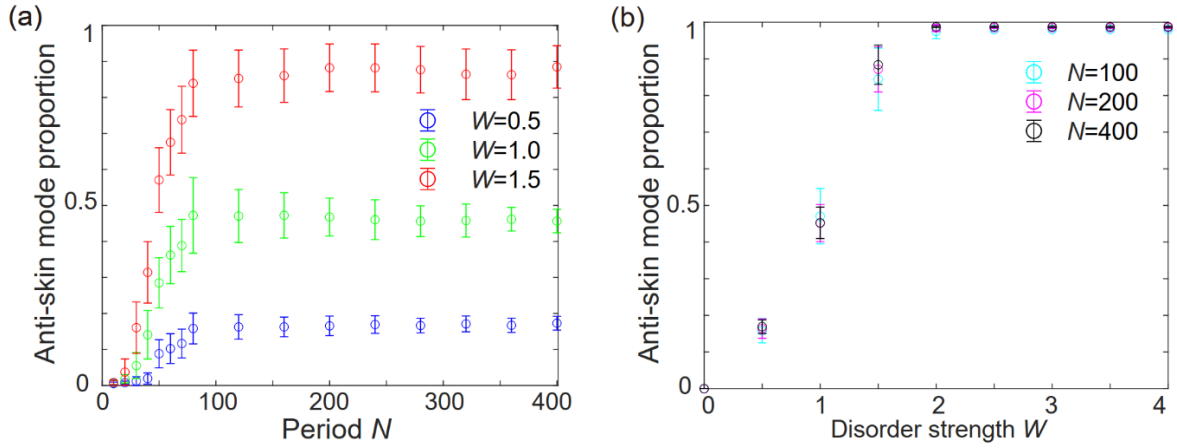


Fig.3 Anti-skin mode proportion in total modes under different period N and disorder amplitude W . Parameters: $t_- = 0.9, t_+ = 1.1, V_{i \text{ mod } N} \in [W, W], L = 400$, sampling times is 100.

Controllable suppression of skin modes in high dimensions --- The NHSEs is closely related to the Anderson localization, but due to the fact the onsite energy distribution is not necessarily random, more means of regulating the skin mode have emerged. When considering the two-dimensional skin mode, adding a similar cosine onsite energy distribution as mentioned above, as shown in Fig.4, we can still observe that the skin mode exhibits a phenomenon of first suppressing the skin modes, then returning to the boundary as p/q increases. Panel Fig .4(d) and 4(e) presenting two and three wave nodes that are not at the chain bisection and trisection points is due to boundary size effects. If continuing to generalize to higher dimensions, we will need to consider the scaling theory in Anderson localization[64]. When the size is infinitely large, all states in one-dimensional and two-dimensional are localized, but there is a critical point in three-dimensional and higher ones. When the disorder is below the critical point, the three-dimensional NHSEs may not be suppressed, but when it is above the critical point, the three-dimensional NHSEs will be completely localized[64]. In the case of cosine distribution, as long as the cosine amplitude continues to increase, its overall disorder strength will also continue to increase until crossing the critical points, all skin modes may be suppressed. Therefore, NHSEs in three-dimensional systems are still constrained by the scaling theory. The difference is that the cosine function distribution can cause more complex association in disorder strength and period, thus better regulation of skin mode suppression, achieving both robustness and tunability of skin modes.

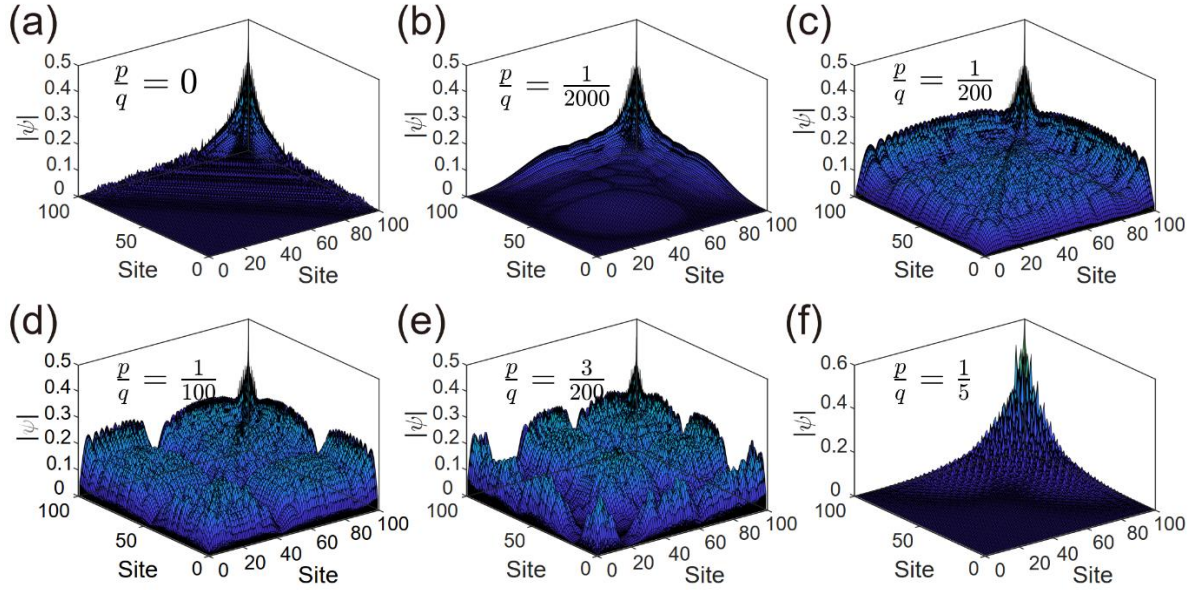


Fig.4 Skin modes suppression in two dimensions. Take 100 atoms with cosine onsite energy distribution applied along both x-axis and y-axis, and calculate state distribution under $t_x^- = 0.9, t_x^+ = 1.1, t_y^- = 0.9, t_y^+ = 1.1$.

The conclusion and discussion --- Starting from the distribution of magnetic fields-like onsite potential energy, this work discovered the non-monotonic suppression patterns of magnetic fields on skin modes. To explain the source of non-monotonic suppression patterns, we also construct random-like potential energy distribution, not only has we gained a profound understanding of the connection and difference between order and disorder, but we have also developed a general strategy to control skin mode suppression. Among them, the relationship between onsite potential energy and magnetic field is universal versus special, and onsite potential energy may have different forms of presentation in different physical fields. Disorder is also not only limited to the disorder of potential energy, but also to disorder in other fields, such as hopping terms. This suppression patterns by order and disorder can be extended to more complex situations. In addition, skin mode suppression cannot be reflected in conventional Generalized Brillouin Zones (GBZs)[70], and it can even be boldly conjecture that all localization cannot be reflected in GBZs[71]. We need to further deepen our research on the impact of localization on skin modes, and find more effective tools to indicate or characterize skin modes.

The work is supported by the National Key R&D Program of China (Grant No. 2021YFA1401100), the National Natural Science Foundation of China (No. 12174293), the Fundamental Research Funds for the Central Universities (No. 2042022kf0047), and the Special Fund of Hubei Yangtze Memory Laboratory.

*Corresponding author.

zhiqiang.guan@whu.edu.cn

- [1]Y. Choi, S. Kang, S. Lim, W. Kim, J.-R. Kim, J.-H. Lee and K. An, Phys. Rev. Lett. **104**, 153601 (2010)
- [2]S. Diehl, E. Rico, M. A. Baranov and P. Zoller, Nature Phys. **7**, 971 (2011)
- [3]E. Persson, I. Rotter, H. J. Stöckmann and M. Barth, Phys. Rev. Lett. **85**, 2478 (2000)
- [4]P. Doyeux, S. A. H. Gangaraj, G. W. Hanson and M. Antezza, Phys. Rev. Lett. **119**, 173901 (2017)
- [5]S. Buddhiraju, A. Song, G. T. Papadakis and S. Fan, Phys. Rev. Lett. **124**, 257403 (2020)
- [6]W. Chen, Ş. Kaya Özdemir, G. Zhao, J. Wiersig and L. Yang, Nature **548**, 192 (2017)
- [7]B. Peng, Ş. K. Özdemir, M. Liertzer, W. Chen, J. Kramer, H. Yilmaz, J. Wiersig, S. Rotter and L. Yang, Proc. Natl. Acad. Sci. **113**, 6845 (2016)
- [8]J. Wiersig, Phys. Rev. Lett. **112**, 203901 (2014)
- [9]A. A. Zyblovsky, A. P. Vinogradov, A. A. Pukhov, A. V. Dorofeenko and A. A. Lisyansky, Physics-Uspekhi **57**, 1063 (2014)
- [10]Ş. K. Özdemir, S. Rotter, F. Nori and L. Yang, Nat. Mater. **18**, 783 (2019)
- [11]V. V. Konotop, J. Yang and D. A. Zezyulin, Rev. Mod. Phys. **88**, 035002 (2016)
- [12]L. Feng, R. El-Ganainy and L. Ge, Nat. Photonics **11**, 752 (2017)
- [13]R. El-Ganainy, K. G. Makris, M. Khajavikhan, Z. H. Musslimani, S. Rotter and D. N. Christodoulides, Nature Phys. **14**, 11 (2018)
- [14]J. Wiersig, Phys. Rev. A **93**, 033809 (2016)
- [15]J. Zhu, S. K. Ozdemir, Y.-F. Xiao, L. Li, L. He, D.-R. Chen and L. Yang, Nat. Photonics **4**, 122 (2010)
- [16]S. Dong, G. Hu, Q. Wang, Y. Jia, Q. Zhang, G. Cao, J. Wang, S. Chen, D. Fan, W. Jiang, Y. Li, A. Alù and C.-W. Qiu, ACS Photonics **7**, 3321 (2020)
- [17]T. Liu, Y.-R. Zhang, Q. Ai, Z. Gong, K. Kawabata, M. Ueda and F. Nori, Phys. Rev. Lett. **122**, 076801 (2019)
- [18]C. H. Lee, L. Li and J. Gong, Phys. Rev. Lett. **123**, 016805 (2019)
- [19]D. S. Borgnia, A. J. Kruchkov and R.-J. Slager, Phys. Rev. Lett. **124**, 056802 (2020)
- [20]K. Kawabata, T. Bessho and M. Sato, Phys. Rev. Lett. **123**, 066405 (2019)
- [21]F. K. Kunst, E. Edvardsson, J. C. Budich and E. J. Bergholtz, Phys. Rev. Lett. **121**, 026808 (2018)
- [22]F. Song, S. Yao and Z. Wang, Phys. Rev. Lett. **123**, 170401 (2019)
- [23]S. Yao, F. Song and Z. Wang, Phys. Rev. Lett. **121**, 136802 (2018)
- [24]S. Yao and Z. Wang, Phys. Rev. Lett. **121**, 086803 (2018)
- [25]N. Okuma, K. Kawabata, K. Shiozaki and M. Sato, Phys. Rev. Lett. **124**, 086801 (2020)
- [26]C.-K. Chiu, J. C. Y. Teo, A. P. Schnyder and S. Ryu, Rev. Mod. Phys. **88**, 035005 (2016)
- [27]M. Z. Hasan and C. L. Kane, Rev. Mod. Phys. **82**, 3045 (2010)
- [28]X.-L. Qi and S.-C. Zhang, Rev. Mod. Phys. **83**, 1057 (2011)
- [29]H. Shen, B. Zhen and L. Fu, Phys. Rev. Lett. **120**, 146402 (2018)
- [30]N. P. Armitage, E. J. Mele and A. Vishwanath, Rev. Mod. Phys. **90**, 015001 (2018)
- [31]E. J. Bergholtz, J. C. Budich and F. K. Kunst, Rev. Mod. Phys. **93**, 015005 (2021)
- [32]K. Zhang, Z. Yang and C. Fang, Nat. Commun. **13**, 2496 (2022)
- [33]K. Zhang, Z. Yang and C. Fang, Phys. Rev. Lett. **125**, 126402 (2020)
- [34]Z. Gong, Y. Ashida, K. Kawabata, K. Takasan, S. Higashikawa and M. Ueda, Phys. Rev. X **8**, 031079 (2018)
- [35]K. Kawabata, K. Shiozaki, M. Ueda and M. Sato, Phys. Rev. X **9**, 041015 (2019)
- [36]D. Leykam, K. Y. Bliokh, C. Huang, Y. D. Chong and F. Nori, Phys. Rev. Lett. **118**, 040401 (2017)
- [37]Y. Xiong, Journal of Physics Communications **2**, 035043 (2018)
- [38]M. Brandenbourger, X. Locsin, E. Lerner and C. Coulais, Nat. Commun. **10**, 4608 (2019)

- [39]T. Hofmann, T. Helbig, F. Schindler, N. Salgo, M. Brzezińska, M. Greiter, T. Kiessling, D. Wolf, A. Vollhardt, A. Kabaši, C. H. Lee, A. Bilušić, R. Thomale and T. Neupert, Phys. Rev. Research **2**, 023265 (2020)
- [40]A. Ghatak, M. Brandenbourger, J. Van Wezel and C. Coulais, Proc. Natl. Acad. Sci. **117**, 29561 (2020)
- [41]K. Wang, A. Dutt, K. Y. Yang, C. C. Wojcik, J. Vučković and S. Fan, Science **371**, 1240 (2021)
- [42]H. Xin, W. Song, S. Wu, Z. Lin, S. Zhu and T. Li, Phys. Rev. B **107**, 165401 (2023)
- [43]Z. Gu, H. Gao, H. Xue, J. Li, Z. Su and J. Zhu, Nat. Commun. **13**, 7668 (2022)
- [44]L. Zhang, Y. Yang, Y. Ge, Y.-J. Guan, Q. Chen, Q. Yan, F. Chen, R. Xi, Y. Li, D. Jia, S.-Q. Yuan, H.-X. Sun, H. Chen and B. Zhang, Nat. Commun. **12**, 6297 (2021)
- [45]D. Zou, T. Chen, W. He, J. Bao, C. H. Lee, H. Sun and X. Zhang, Nat. Commun. **12**, 7201 (2021)
- [46]L. Xiao, T. Deng, K. Wang, G. Zhu, Z. Wang, W. Yi and P. Xue, Nat. Phys. **16**, 761 (2020)
- [47]M.-J. Liao, M.-S. Wei, Z. Lin, J. Xu and Y. Yang, Results in Physics **57**, 107372 (2024)
- [48]X.-R. Ma, K. Cao, X.-R. Wang, Z. Wei, Q. Du and S.-P. Kou, Phys. Rev. Research **6**, 013213 (2024)
- [49]X. Zhang, T. Zhang, M.-H. Lu and Y.-F. Chen, Advances in Physics: X **7**, 2109431 (2022)
- [50]S.-Q. Wu, Y. Xu and J.-H. Jiang, Frontiers in Physics **11**, 1123596 (2023)
- [51]Y. Peng, J. Jie, D. Yu and Y. Wang, Phys. Rev. B **106**, L161402 (2022)
- [52]M. Lu, X.-X. Zhang and M. Franz, Phys. Rev. Lett. **127**, 256402 (2021)
- [53]C.-X. Guo, C.-H. Liu, X.-M. Zhao, Y. Liu and S. Chen, Phys. Rev. Lett. **127**, 116801 (2021)
- [54]Z. Fang, M. Hu, L. Zhou and K. Ding, Nanophotonics **11**, 3447 (2022)
- [55]Y.-C. Wang, J.-S. You and H. H. Jen, Nat. Commun. **13**, 4598 (2022)
- [56]C.-A. Li, B. Trauzettel, T. Neupert and S.-B. Zhang, Phys. Rev. Lett. **131**, 116601 (2023)
- [57]D. R. Hofstadter, Phys. Rev. B **14**, 2239 (1976)
- [58]P. Streda, J. Phys. C: Solid State Phys. **15**, L717 (1982)
- [59]G. H. Wannier, Phys. Status Solidi (B) **88**, 757 (2006)
- [60]J. Zak, Phys. Rev. **134**, A1602 (1964)
- [61]R. Peierls, Zeitschrift für Physik **80**, 763 (1933)
- [62]D. J. Thouless, M. Kohmoto, M. P. Nightingale and M. Den Nijs, Phys. Rev. Lett. **49**, 405 (1982)
- [63]P. W. Anderson, Phys. Rev. **109**, 1492 (1958)
- [64]E. Abrahams, P. W. Anderson, D. C. Licciardello and T. V. Ramakrishnan, Phys. Rev. Lett. **42**, 673 (1979)
- [65]D. J. Thouless, J. Phys. C: Solid State Phys. **3**, 1559 (1970)
- [66]N. Mott, J. Phys. C: Solid State Phys. **20**, 3075 (1987)
- [67]H. Jiang, L.-J. Lang, C. Yang, S.-L. Zhu and S. Chen, Phys. Rev. B **100**, 054301 (2019)
- [68]J. Claes and T. L. Hughes, Phys. Rev. B **103**, L140201 (2021)
- [69]R. Sarkar, S. S. Hegde and A. Narayan, Phys. Rev. B **106**, 014207 (2022)
- [70]K. Yokomizo and S. Murakami, Phys. Rev. Lett. **123**, 066404 (2019)
- [71]R. Abou-Chacra, D. J. Thouless and P. W. Anderson, J. Phys. C: Solid State Phys. **6**, 1734 (1973)

Supplemental Material for " A general strategy to control suppression of Non-Hermitian skin effects "

Chao Xu¹, Zhiqiang Guan^{1,2,3,4*} and Hongxing Xu^{1,2,4*}

¹ School of Physics and Technology, Center for Nanoscience and Nanotechnology, and Key Laboratory of Artificial Micro- and Nano-structures of Ministry of Education, Wuhan University, Wuhan 430072, China

²School of Microelectronics, Wuhan University, Wuhan 430072, China

³Hubei Yangtze Memory Laboratories, Wuhan 430205, China

⁴Wuhan Institute of Quantum Technology, Wuhan 430206, China

I Non-Hermitian Hofstadter model	10
II The suppression of non-Hermitian skin effects in Hofstadter model.....	11
III Skin modes anomyly in triangle onsite energy distribution.....	13
IV Wavefunction distribution under disorder	14

I Non-Hermitian Hofstadter model

The Hofstadter model was originally derived from the problem of calculating the energy spectrum of a single electron in a square lattice with a vertical magnetic field applied. The core feature of the Hofstadter model is the possession of a magnetic translation group, the Peierls substitution is taken along the x-axis direction, the magnetic flux per unit cell $\phi = 2\pi \frac{p}{q}$, where p,q are coprime, t_x is the x-axis direction nearest-neighbor hopping amplitude, t_y^- and t_y^+ are the y-axis direction nearest-neighbor downward and upward hopping amplitudes, and the Hamiltonian can be written as

$$\hat{H} = \sum_{m,n} (t_x \hat{c}_{m+1,n}^\dagger \hat{c}_{m,n} e^{i\phi n} + t_x \hat{c}_{m,n}^\dagger \hat{c}_{m+1,n} e^{-i\phi n} + t_y^+ \hat{c}_{m,n+1}^\dagger \hat{c}_{m,n} + t_y^- \hat{c}_{m,n}^\dagger \hat{c}_{m,n+1}) \quad (S1)$$

Non-reciprocal hoppings do not break the magnetic translation group. If the y-axis direction is taken as reciprocal nearest neighbor hoppings, i.e., $t_y^- = t_y^+$, there will be q zero-energy Dirac points protected by the hidden chiral symmetry when q is even. In our choosing parameters, both Hermitian and non-Hermitian system can realize the topological edge states when the y-axis is taken as OBCs, while the bulk states of non-Hermitian ones converge to the edges as shown in Fig. 1(d).

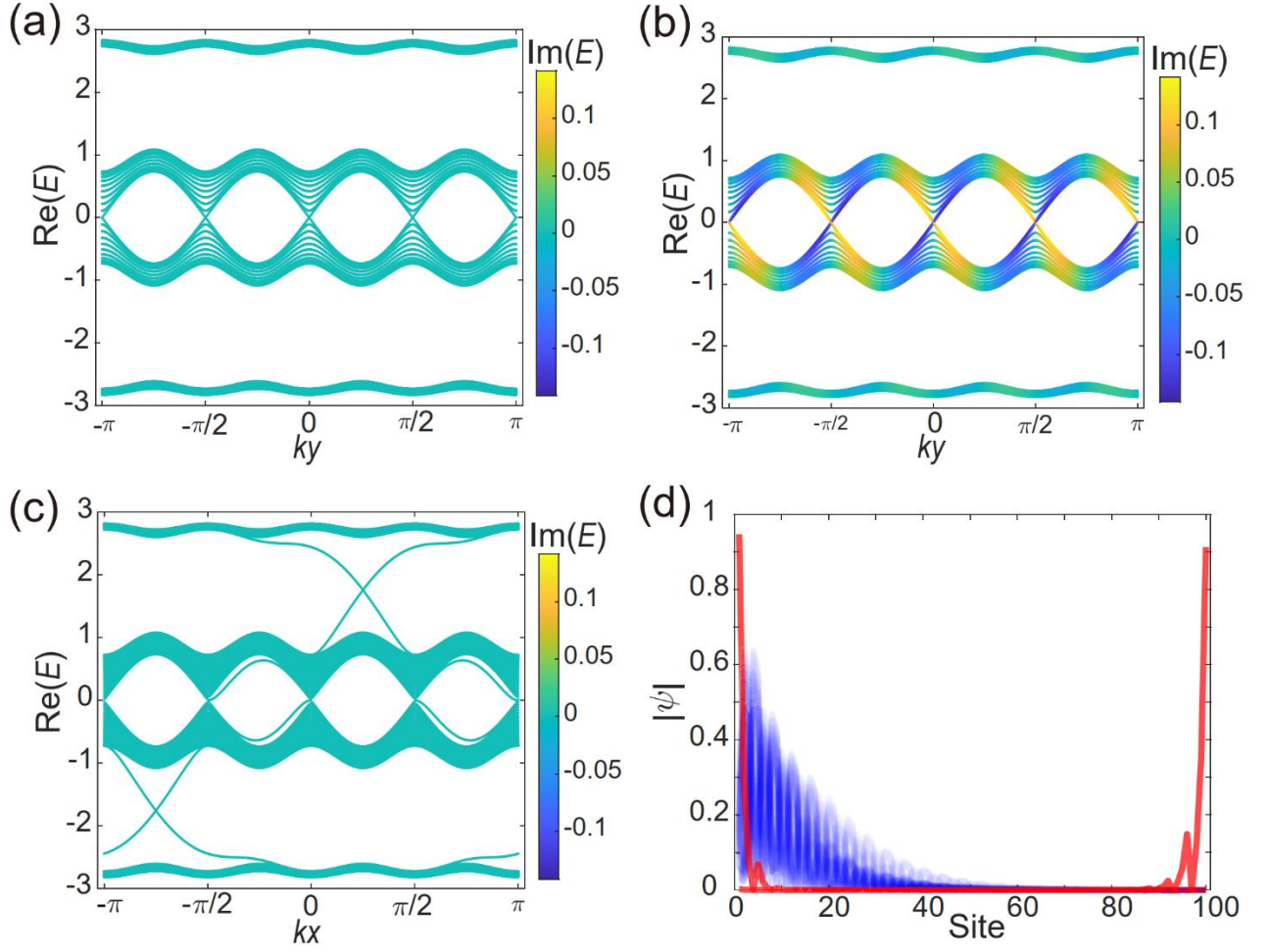


Fig. 1 Non-Hermitian Hofstadter model. (a), (b) are the projected energy bands for $p=1$, $q=4$ taking periodic boundary conditions at both directions, where (a), (b) nearest neighbor hoppings are $t_x = t_y^- = t_y^+ = 1$ and $t_x^- = 1.1, t_y^+ = 0.9$, respectively. (c) is the projected energy band along the x -axis direction, y -direction takes open boundary conditions (100 atoms in the y -axis). (d) is the distribution of bulk states (in black) and edge states (in red) in (c) for $k_x = \frac{\pi}{4}$.

II The suppression of non-Hermitian skin effects in Hofstadter model

Hermitian Hofstadter models often have non-trivial Chern numbers and may still have non-trivial Chern numbers when making their nearest neighbor hoppings non-reciprocal. Fig. 1(d) is the state distribution including both topological edge states and skin modes. The next step is to study the state distribution under different p and q in the magnetic flux $\phi = 2\pi\frac{p}{q}$. The Hamiltonian is like Eq. 2 in the main text, let $t_x = t_y^- = t_y^+ = 1$, the number of atoms on the y -axis under the OBCs is 500, the projected energy bands of different combinations of p and q in the x -axis direction are calculated

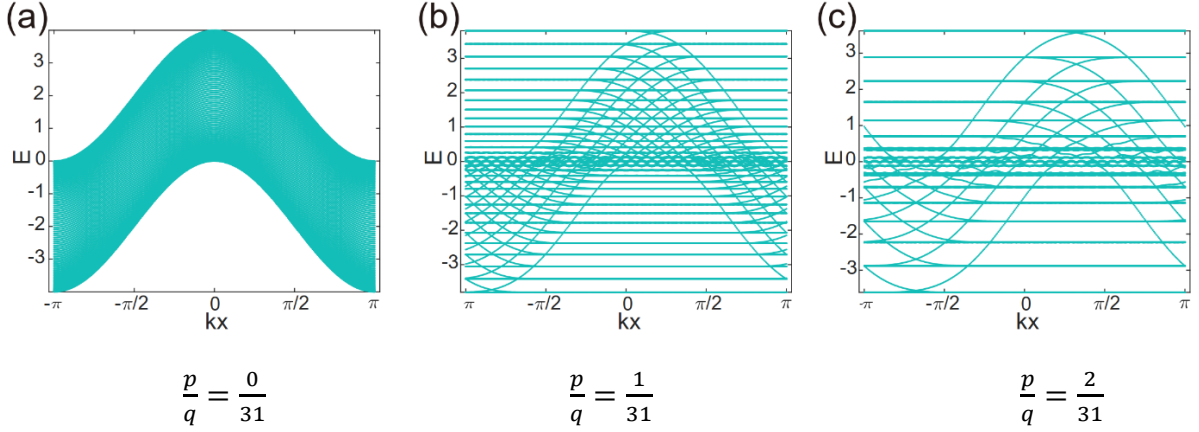


Fig.2 Projected energy bands of the two-dimensional Hermitian Hofstadter model under the OBCs (number of atoms $L=500$) along the y -axis direction and PBCs along the x -axis direction for different magnetic fluxes.

p and q are $\frac{p}{q} = \frac{0}{31}$, $\frac{p}{q} = \frac{1}{31}$, $\frac{p}{q} = \frac{2}{31}$ in (a), (b), and (c), respectively.

The reasonable setting of simulation parameters can make the topological edge states only appear on one side. Take $k_x = 0$ below and calculate state distribution under $t_x = t_y^- = t_y^+ = 1$ and $t_x = 1, t_y^- = 0.9, t_y^+ = 1.1$, respectively.

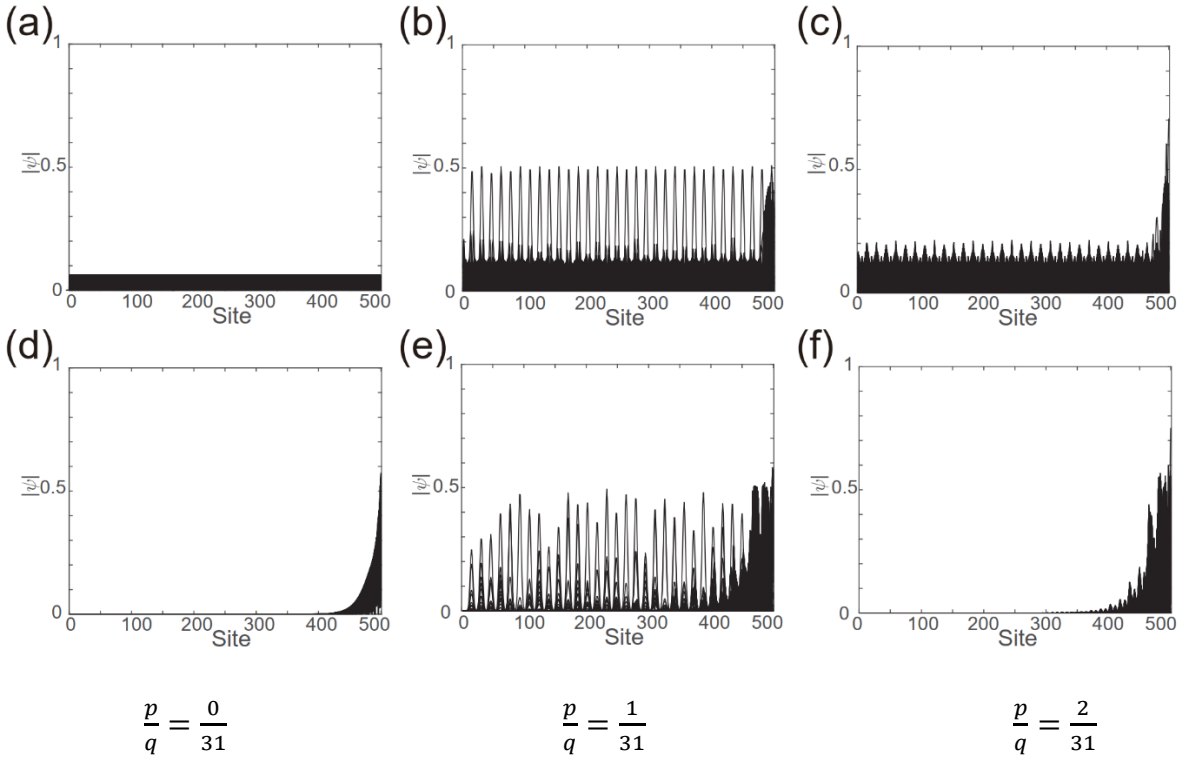


Fig.3 State distribution in Hofstadter model under OBCs with different magnetic field intensities. Take $k_x = 0$ and calculate state distribution under $t_x = t_y^- = t_y^+ = 1$ in (a), (b), (c) and $t_x = 1, t_y^- =$

$0.9, t_y^+ = 1.1$ in (d), (e), (f), respectively. The parameters of p, q in (a), (d) are $\frac{p}{q} = \frac{0}{31}$, ones in (b), (e) are

$\frac{p}{q} = \frac{1}{31}$, ones in (c), (f) are $\frac{p}{q} = \frac{2}{31}$.

Fig. 3 shows that it is possible to generate a topological edge states in the system when adding a magnetic field. If non-reciprocal hopping strength is considered, the concentration degree of the topological edge states will also be affected to a certain extent, but what is more interesting is that when we focus on the bulk states, it is found that when there is no magnetic field at all, the skin depth of the skin modes is very small. However, some skin modes return to the bulk when a weak magnetic field appears. The skin modes concentrate at the boundary when the magnetic field is further strengthened. The suppression pattern of skin modes is very unexpected.

III Skin modes anomly in triangle onsite energy distribution

As mentioned above, the state distribution of projected energy band of the Non-Hermitian Hofstadter model with applied magnetic field is equivalent to the ones of 1D monoatomic chain added the onsite energy with cosine distribution. If we make the onsite energy exhibit a trigonometric distribution, that is, if the site number i satisfies $0 \leq \left\{i * \frac{p}{q}\right\} \leq \frac{1}{2}$, then set $V_i = \left\{i * \frac{p}{q}\right\}$; If $\frac{1}{2} < \left\{i * \frac{p}{q}\right\} < 1$, then set $V_i = 1 - \left\{i * \frac{p}{q}\right\}$. $\left\{i * \frac{p}{q}\right\}$ is the decimal part of $i * \frac{p}{q}$. As above, select an open chain of 500 atoms and calculate the distribution of states with increasing p/q , as shown in Fig. 4. The skin mode are very similar with ones of cosine distribution, showing the characteristic of skin mode first suppressing and then re-skin. This also demonstrates the complex relationship between period and disorder degree, which does not only exist in magnetic fields.

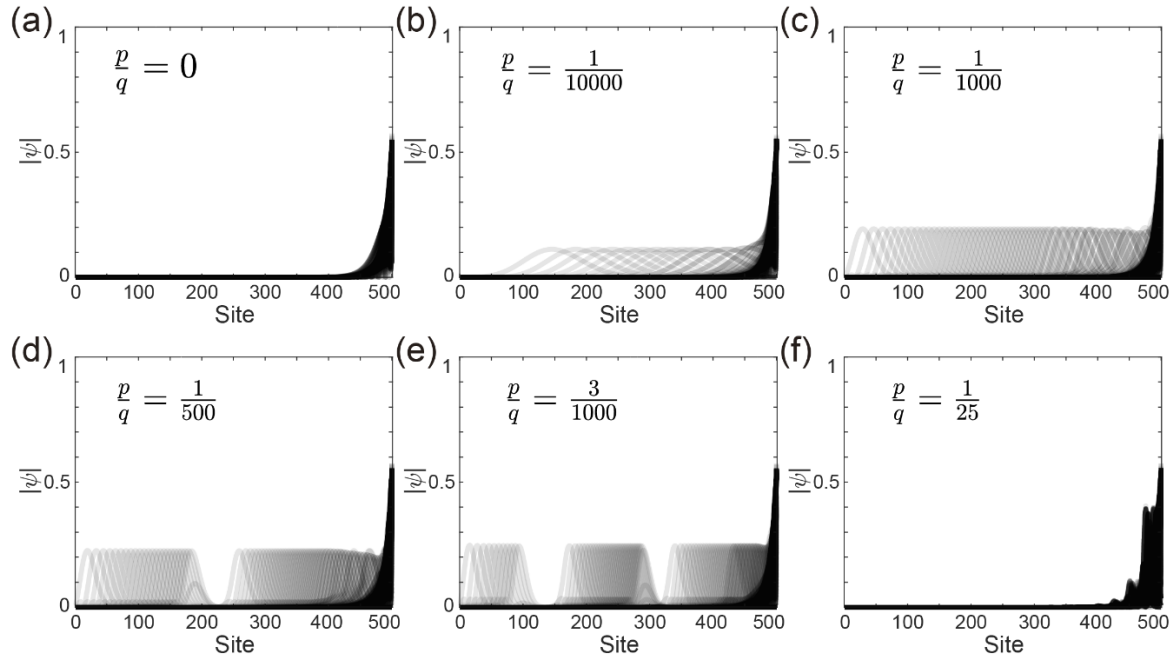


Fig.4 Skin modes anomly in triangle onsite energy distribution. Take 500 atoms in the a 1D monoatomic chain, and calculate state distribution under $t_- = 0.9, t_+ = 1.1$.

IV Wavefunction distribution under disorder

In a one-dimensional atomic chain, when only considering nearest neighbor non-reciprocal hoppings, the bulk state will be localized to the boundary. When an atomic chain is subjected to external disturbances and introduced additional onsite energy, due to topological protection, the bulk state will also tend to the boundary. But when the disorder is large enough, the bulk states may all return to the body due to Anderson localization. The main text has already discussed two variables related to disorder strength, but has not provided a more detailed wavefunction distribution. We follow the same approach to calculate the impact of different period N on the wavefunction. We should try our best to maintain the same variance of the random onsite energy distribution in space. As shown in Fig.5, when the total number of atoms L is 400, there is a general trend of greater period and stronger disorder strength. Due to the significant boundary size effects, the anti-skin mode does not fully exhibit a periodic distribution in space. Continuing to calculate the distribution of the skin mode with a total number of atoms of 2000, it can be seen more clearly that the spatial distribution of the skin mode is more regular. The proportion of anti-skin modes also increases with the increase of period N .

We can have a thought experiment, considering $N = 1$ and $N = L$, two limit cases, which correspond to the Hatano-Nelson model with constants potential energy and the conventional Anderson model, respectively. When N is in a continuously increasing process, it is actually a process of transforming between two models. The disorder strength of this process is positively correlated with the period.

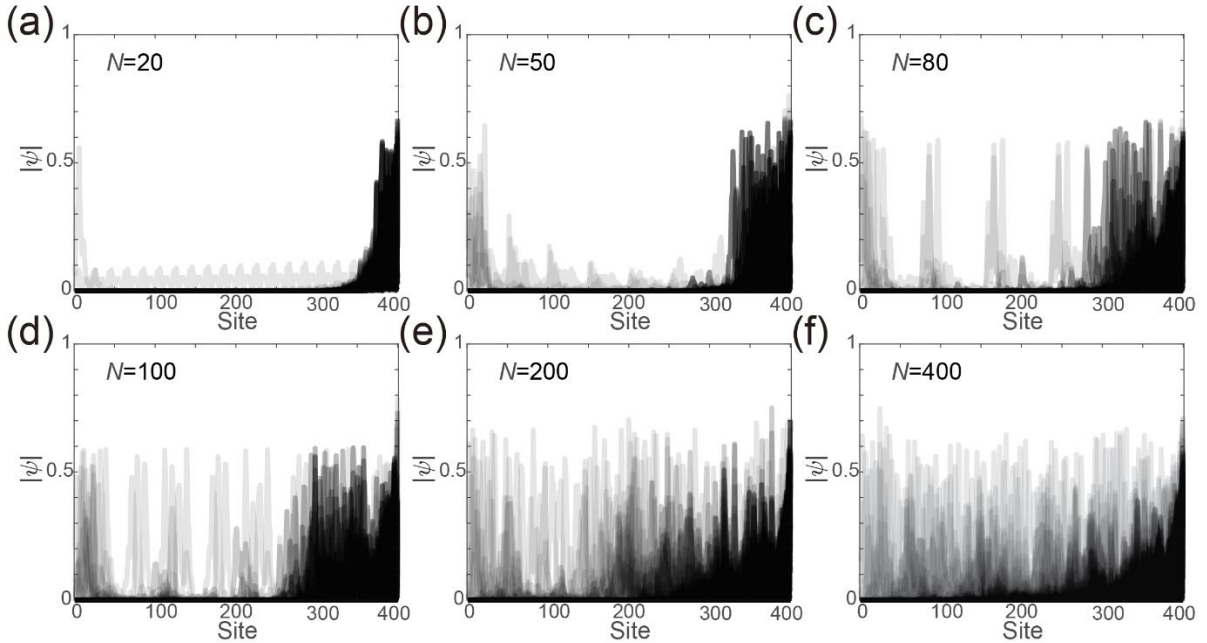


Fig.5 Wavefunction distribution under different period N with whole site number $L = 400$. Parameters: $t_- = 0.9, t_+ = 1.1, V_{i \bmod N} \in [W, W], W = 1$.

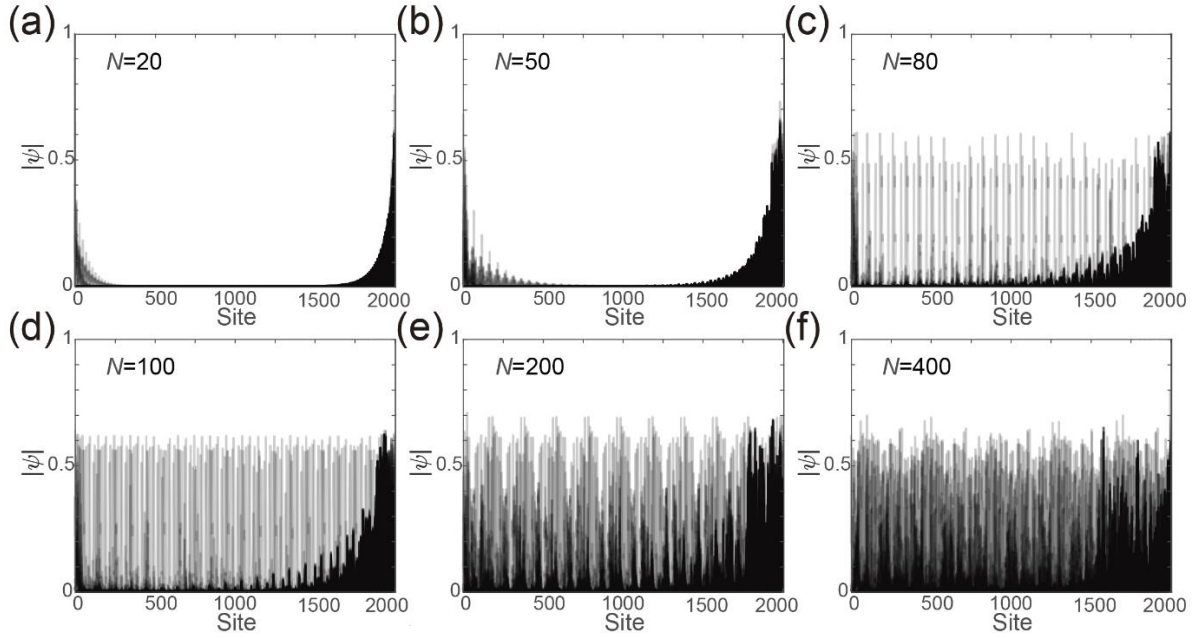


Fig.6 Wavefunction distribution under different period N whole site number $L = 2000$. Parameters: $t_- = 0.9, t_+ = 1.1, V_{i \bmod N} \in [W, W], W = 1$.

Then, Continuing to explore the influence of random onsite energy distribution amplitudes. We chose a chain with a total length of 1000 atoms and started taking periodic boundary conditions, drawing the energy band on the complex plane. It can be seen as the disorder degree increases, the enclosed internal space gradually decreases until it disappears, and this transition point is called the Anderson transition point. This transition point cannot be derived from Generalized Brillouin Zones. Next, we have drawn the state distribution of 100 atoms under three representative disordered intensities under open boundary conditions, and we can see how the skin mode slowly returns to the body.

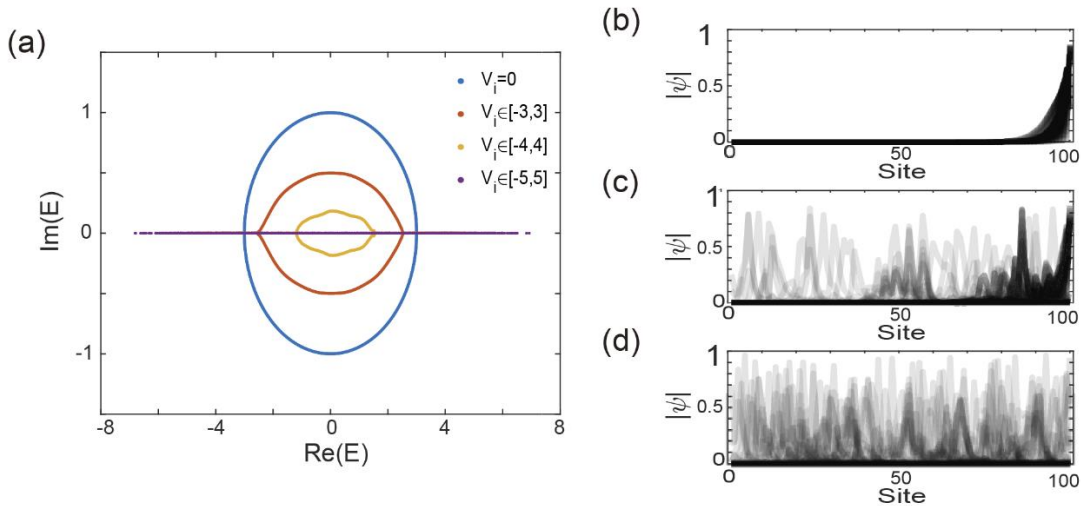


Fig.7 Wavefunction distribution under different disorder amplitude. (a) is the complex spectra with parameters $t_- = 1, t_+ = 2$, subject to random real onsite energies under the periodic boundary conditions (atom numbers $L=1000$), V_i is the random onsite energies on site i . Panel (b), (c), (d) are state distribution when $V_i = 0, V_i \in [-3,3], V_i \in [-5,5]$ in panel (c).